

Some new results on the coding of pheromone intensity in an olfactory sensory neuron

A. Vermeulen^{1,2}, J.-P. Rospars¹, P. Lánský^{3,1}, H.C. Tuckwell^{4,1}

¹ *Laboratoire de Biométrie, Institut National de la Recherche Agronomique
Route de Saint-Cyr, F-78026 Versailles Cedex, France*

² *Laboratoire de Traitement d'Images et Reconnaissance de Formes, Institut
National Polytechnique, 46 Av. Félix Viallet, F-38031 Grenoble Cedex, France*

³ *Institute of Physiology, Academy of Sciences of the Czech Republic
Videnská 1083, 142 20 Prague 4, Czech Republic*

⁴ *School of Mathematical Sciences, Centre for Mathematics and Its Applications,
Australian National University, Canberra, ACT 0200, Australia*

Abstract. Firstly, the effect of a neuron's spatial structure on the dependency of the receptor potential for a constant pheromone-dependent conductance is studied. It is shown that the ability to discriminate is improved by considering a cable model instead of a point model neuron. Secondly, we compare the firing frequency when the passive backpropagation of action potentials is ignored [2,4] with the frequency when this backpropagation is included. For certain sets of parameters, the inclusion of backpropagation has little effect.

1. Introduction

Modeling the sex-pheromone neuroreceptor is a good starting point to develop a biophysical model of single neurons because its dendritic structure is simple [1]. Pheromone coding begins by *transduction* which occurs in the dendrite. The binding of pheromone molecules to receptor proteins borne by the membrane triggers a second-messenger system which finally opens pheromone-dependent ionic channels. Then, a membrane depolarization, called *receptor potential*, is evoked. When this potential is high enough, *action potentials* are generated and propagated along the axon to the brain. We proposed a model [2] describing this sequence of events composed of three functional modules: the *transduction*, *receptor potential* and *action potential* modules. The membrane of the neuroreceptor is modeled by a cylindrical cable which is divided in two parts (Fig. 1), (i) a pheromone-sensitive dendrite containing transduction mechanisms, and (ii) a pheromone-insensitive part corresponding to passive dendrite, soma, initial segment and axon.

In the present work, we focus our attention on the receptor and action potential modules. The pheromone concentration is assumed to be constant. Consequently, the transduction module is in a steady-state and the number of open pheromone-dependent ionic channels is constant. These open channels are modeled by a constant pheromone-dependent conductance Δg^* which is considered here as the input signal of the receptor potential module. Two main problems are studied.

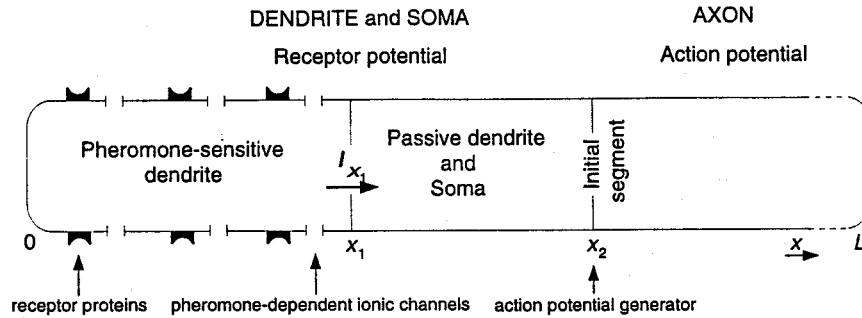


Figure 1. Schematic representation of the sex-pheromone neuroreceptor.

(i) Experimental observations show that the range of variation of the receptor potential in the sex-pheromone neuroreceptor extends over more than 6 decades of pheromone concentration [1]. However, we show that in a point model neuron the range extends over only $2\frac{1}{2}$ decades of the conductance change Δg^* . Can this coding range be increased by taking into account the spatial extension of the neuron?

(ii) In previous work [2,4], we described a model which allowed us to determine analytically the dependency of the firing frequency on the conductance Δg^* without considering the passive backpropagation of the action potential into the dendrite. Is backpropagation really negligible? To answer this question we determine numerically the conductance-frequency relation in the case of backpropagation and compare it to the relation found analytically.

2. Receptor potential for different spatial structures

The receptor potential module is based on a cable model of the neuron [5] in which each area of membrane behaves as the electric circuit shown in Fig. 2 with membrane resistance r_m of unit length times unit length, membrane capacitance c_m per unit length, resistance of internal medium r_i per unit length, pheromone-dependent conductance $\Delta g(x)$ (in units of r_m^{-1}) and reversal potential E of the pheromone-dependent conductance. The receptor potential $V(x)$ of the steady-state cable is described by an ordinary differential equation (ODE)

$$-\frac{d^2 V(x)}{dx^2} + V(x) = \Delta g(x) (E - V(x)), \quad 0 < x < L, \quad (1)$$

where L is the length of the neuron and x the distance along the neuron expressed in units of the characteristic length λ ($= \sqrt{r_m/r_i}$). We will find solutions of this equation for various cable lengths when the conductance $\Delta g(x)$ is a positive constant over the pheromone-sensitive dendrite and zero elsewhere

$$\Delta g(x) = \Delta g^* (1 - H(x - x_1)), \quad 0 \leq x \leq L, \quad (2)$$

where $H(x)$ is the unit (Heaviside) step function and x_1 ($0 < x_1 < L$) corresponds to the border between the pheromone-sensitive dendrite and pheromone-

insensitive part (Fig. 1).

The solution of equation (1) may be calculated by using the input resistance of the pheromone-insensitive part. The general solution of (1) on $[0, x_1]$ with conductance (2) for the pheromone-sensitive dendrite is given by

$$V(x) = c_1 \sinh(\alpha x) + c_2 \cosh(\alpha x) + \frac{\Delta g^* E}{\Delta g^* + 1}, \quad 0 \leq x \leq x_1, \quad (3)$$

where $\alpha = \sqrt{1 + \Delta g^*}$, c_1 and c_2 are constants to be determined by using the boundary conditions at the beginning ($x = 0$) and end ($x = x_1$) of the pheromone-sensitive dendrite. By considering that no current flows at $x = 0$, the so called "sealed end" condition (see [5]), and that there is conservation of axial current I_{x_1} at $x = x_1$ (Fig. 1), the boundary conditions may be written as

$$V'(0) = 0, \quad \text{and} \quad V'(x_1) = -r_i I_{x_1}. \quad (4)$$

where ' indicates differentiation with respect to x . The current I_{x_1} can be computed knowing the input resistance R_{in} ($= V(x_1)/I_{x_1}$ by definition) of the pheromone-insensitive part

$$I_{x_1} = \frac{V(x_1)}{R_{in}}. \quad (5)$$

Combining equations (3), (4) and (5) give

$$V(x) = \left(1 - \frac{\cosh(\alpha x)}{\beta \alpha \sinh(\alpha x_1) + \cosh(\alpha x_1)}\right) \frac{\Delta g^* E}{\Delta g^* + 1}, \quad 0 \leq x \leq x_1, \quad (6)$$

with $\beta = R_{in}/r_i$. The required input resistance (and hence the receptor potential on the pheromone-insensitive part) can be found in table 4.2 of [5] for different types of boundary conditions.

Case (i). Finite L. Considering the pheromone-insensitive part as a finite cable with a sealed end at L , the input resistance is given by $R_{in} = r_i \coth(L - x_1)$ and the receptor potential by

$$V(x) = \begin{cases} \left(1 - \frac{\cosh(\alpha x)}{\alpha \coth(L - x_1) \sinh(\alpha x_1) + \cosh(\alpha x_1)}\right) \frac{\Delta g^* E}{\Delta g^* + 1}, & 0 \leq x \leq x_1, \\ V(x_1) \cdot \frac{\cosh(L - x)}{\cosh(L - x_1)}, & x_1 < x \leq L. \end{cases} \quad (7)$$

Case (ii). $L = \infty$. In the original model [2] we considered the pheromone-insensitive part as a semiinfinite cable ($L = \infty$) so the input resistance is given by $R_{in} = r_i$ and the receptor potential by

$$V(x) = \begin{cases} \left(1 - \frac{\cosh(\alpha x)}{\alpha \sinh(\alpha x_1) + \cosh(\alpha x_1)}\right) \frac{\Delta g^* E}{\Delta g^* + 1}, & 0 \leq x \leq x_1, \\ V(x_1) \cdot \exp(-(x - x_1)), & x > x_1. \end{cases} \quad (8)$$

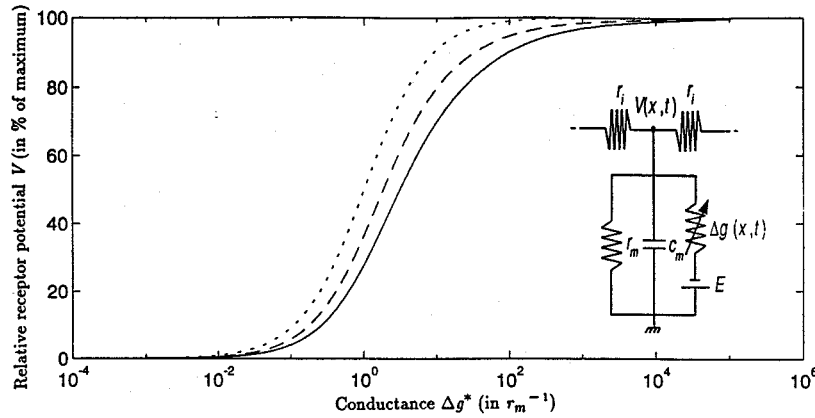


Figure 2. Receptor potential for different spatial structures. Relative receptor potential at the initial segment as a function of the conductance Δg^* for a point model neuron ($\cdot \cdot \cdot$), a finite cable with sealed end at $L = 1.5\lambda$ ($---$) and a semiinfinite cable ($—$). In the last two cases, $x_1 = \lambda$. Electric circuit illustrates the receptor potential module.

The dependence of the relative receptor potential at the initial segment x_2 ($x_1 < x_2 < L$) on the conductance Δg^* for (8) is shown in Fig. 2. For comparison the same relation is shown for a point model neuron ($d^2 V(x)/dx^2 = 0$ in (1)) and a finite cable (7) with sealed end at $L = 1.5\lambda$. It is found that the potential changes less rapidly when the spatial extension of the neuron is taken into account. More precisely, in the 5-95% interval of the relative receptor potential, the range of Δg^* is 2.6 decades (point model neuron), 3.1 decades (short finite cable) and 3.5 decades (semiinfinite cable). Thus, the difference is approximately one decade when a long cable is considered instead of a simple point model neuron. This means that an extended neuron can code over a wider range of the input signal.

3. Backpropagation of action potential into dendrite

In [2, 4], we assume no backpropagation of the action potential into the dendrite. This simplification allows us to determine analytically the firing frequency f as a function of the steady-state receptor potential $V(x_2)$. In order to do this, the action potential module is based on a simplified phenomenological model. The potential of the initial segment $V_{IS}(t)$ is modeled by the electric circuit shown in Fig. 3B. It is characterized by a switch which simulates the action potential generation and a current source $I = V(x_2)/r_m$ which simulates the current coming from other parts of the neuron. If the potential $V_{IS}(t)$ exceeds the firing threshold θ , an action potential is triggered and the switch is closed for a period corresponding to the absolute refractory period T_{ref} . The dependency of the firing frequency f on the potential $V(x_2)$ is given by,

$$f = \left\{ \ln \left(\frac{V(x_2)}{V(x_2) - \theta} \right) + T_{ref} \right\}^{-1}, \quad V(x_2) > \theta. \quad (9)$$

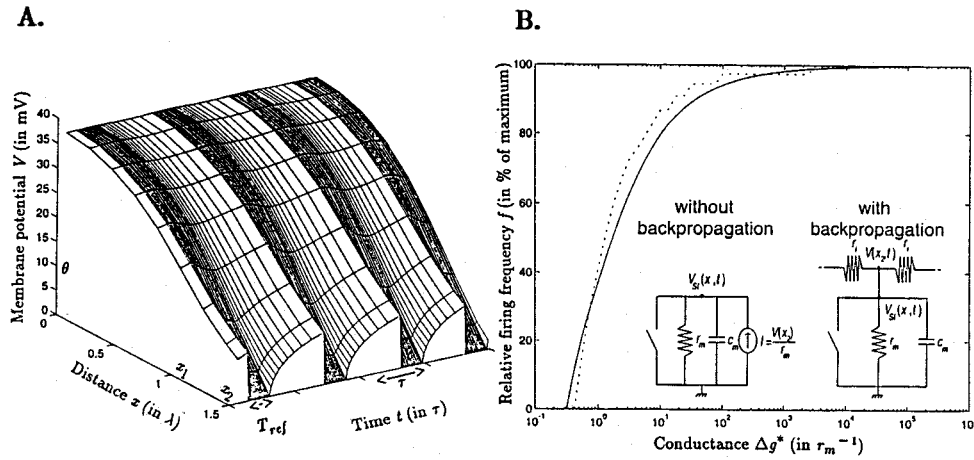


Figure 3. Backpropagation of action potential into dendrite. **A.** Example of the profile of the membrane potential $V(x, t)$ between the beginning of the cable and the initial segment x_2 for $\Delta g^* = 1$. **B.** Relative firing frequency as a function of the conductance Δg^* with (· · ·) and without (—) backpropagation. Electric circuits illustrating the action potential module with and without backpropagation. Both figures were calculated with $x_1 = \lambda$, $x_2 = 1.5\lambda$, $\theta = 10$ mV, $E = 100$ mV and $T_{ref} = \frac{\tau}{6}$.

Using the value of $V(x_2)$ from (8) in equation (9) to replace $V(x_2)$, we obtain an analytical solution for the dependency of the firing frequency f on the conductance Δg^* .

We now compare this analytical solution with a numerical solution for a more realistic model where the passive backpropagation of the action potential into the dendrite is permitted. This is done by introducing a switch at the initial segment x_2 . In this way the generation of an action potential influences the membrane potential along the cable. Hence, the membrane potential is no longer described by the receptor potential alone and we have to replace the steady-state cable (1) by a time-dependent cable which is described by the partial differential equation

$$-\frac{\partial^2 V(x, t)}{\partial x^2} + \frac{\partial V(x, t)}{\partial t} + V(x, t) = \Delta g(x, t)(E - V(x, t)), \quad 0 < x < L, \quad (10)$$

with time t expressed in time constant units $\tau (= r_m c_m)$.

No analytical solution of (10) is known for the chosen input signal (2), so the equation is solved numerically. The spatial discretisation is performed using finite differences, and the method of lines is employed to reduce (10) to a system of coupled ODEs. This system is then integrated forward using the implicit Euler method with an adaptive step size, as in [6], to avoid numerical instabilities or oscillations [3].

An example of the profile of the membrane potential $V(x, t)$ from the

beginning of the cable to the initial segment x_2 is shown in Fig. 3A. The dependency of the relative firing frequency on the conductance Δg^* is shown in Fig. 3B and compared with the analytical solution without backpropagation of action potentials. It may be concluded for the present model, that in the case studied, the firing frequency is relatively independent of the backpropagation of the action potentials.

4. Conclusions and perspectives

In conclusion, the results presented can be summarized as follows. (i) As far as coding performance is considered, the spatial extension of a neuron is a significant feature. This is shown by a wider coding range of the pheromone-dependent conductance for a spatially extended neuron than for a point model neuron. This conclusion is interesting because the point model neuron is a commonly used neuron model. (ii) Conversely, the passive backpropagation of the action potentials into the dendrite does not seem to have much influence on the firing frequency. At least in the case studied, it seems that the receptor potential is not modified by the backpropagation of spikes.

These properties will be investigated further by a more systematic study of the influence of the geometric parameters (x_1 , x_2 , L). Then, the model will be extended to more realistic neural geometries; numerical methods will be used to study for instance the influence of the different diameters of the various neuron parts (dendrite, soma, axon). The evolution of the receptor potential for space-dependent and time-dependent conductance $\Delta g(x, t)$ will also be considered.

References

1. K.E. Kaissling: *R.H. Wright lectures on insect olfaction*. K. Colbow (ed.), Simon Fraser University, Burnaby, Canada (1987)
2. P. Lánský, J.-P. Rospars, A. Vermeulen: Basic mechanisms of coding stimulus intensity in the olfactory sensory neuron. *Neural Processing Letters*, 1, 9-13 (1994)
3. M.V. Mascagni: Numerical methods for neuronal modeling. In *Methods in neural modeling : from synapses to networks*, C. Koch, I. Segev (eds.), A Bradford Book, The MIT Press, Cambridge, Massachusetts, London (1989)
4. J.-P. Rospars, P. Lánský, H.C. Tuckwell, A. Vermeulen: Coding odor intensity in a deterministic model of first-order olfactory neurons (in preparation)
5. H.C. Tuckwell: *Introduction to theoretical neurobiology*, Vol. 1. Cambridge University Press, Cambridge (1988)
6. J. White, K.A. Hamilton, S.R. Neff, J.S. Kauer: Emergent properties of odor information coding in a representational model of the salamander olfactory bulb. *The Journal of Neuroscience*, 12, 1772-1780 (1992)